

**EVALUATION OF ASPECTS OF E\* TEST USING HMA SPECIMENS WITH  
VARYING VOID CONTENTS**

Geoffrey M. Rowe, Ph.D., PE  
Abatech, Inc.  
PO Box 356  
Blooming Glen, PA 18911  
Phone: (215) 258-3640  
Fax: (772) 679-2464  
growe@abatech.com

Salman Hakimzadeh  
Graduate Research Student  
University of KY  
161 Oliver Raymond Building  
University of Kentucky  
Lexington, KY  
Phone: (859) 351-1331  
shakimzadeh@uky.edu

Phillip Blankenship, PE  
Asphalt Institute  
2696 Research Park Drive  
Lexington, KY 40511  
Phone: (859) 288-4986  
Fax: (859) 299-4999  
pblankenship@asphaltinstitute.org

November 2008

WORDS: 2995  
FIGURES: 12x250 = 3000  
TABLES: 6x250 = 1500  
TOTAL: 7495

## **EVALUATION OF ASPECTS OF E\* TEST USING HMA SPECIMENS WITH VARYING VOID CONTENTS**

### **ABSTRACT**

A dynamic modulus master curve for asphalt concrete is a critical input for flexible pavement design in the mechanistic-empirical pavement design guide developed in NCHRP Project 1-37A which has drawn much attention among asphalt technologists. The objectives in this study are to, 1) consider and compare different analysis techniques for construction of the master curve, and 2) measure and analyze the effect of permanent strain on samples that have been tested using the SPT modulus test. It was found that differences existed in the values of calculated asymptote values and shape of master curve depending upon which method was adopted. Recommendations are made for modifications to the testing protocol and further work to determine the effect of permanent strain at higher test temperatures.

## EVALUATION OF ASPECTS OF E\* TEST USING HMA SPECIMENS WITH VARYING VOID CONTENTS

Geoffrey M. Rowe, Salman Hakimzadeh, and Phillip Blankenship

### INTRODUCTION

The dynamic modulus of an asphalt mixture is a significant parameter that determines the ability of material to resist compressive deformation as it is subjected to cyclic compressive loading and unloading. The dynamic modulus test has been suggested by NCHRP Projects 9-19 and 9-29 as a simple performance test (SPT) to verify the performance characteristics of Superpave mixture designs (1). It has also been suggested as the potential quality control-quality assurance parameter in the field (2). Dynamic modulus is also an input to the Mechanistic-Empirical Pavement Design guide (MEPDG) (3) and supports the predictive performance models developed as part of NCHRP project 1-37A (4).

For visco-elastic materials such as HMA mixtures, the stress-strain relationship under a continuous sinusoidal loading is defined by its complex dynamic modulus ( $E^*$ ). This is a complex number that relates stress to strain for linear visco-elastic materials subjected to continuously applied sinusoidal loading in the frequency domain. The complex modulus is defined as the ratio of the amplitude of the sinusoidal stress and the amplitude of the sinusoidal strain, as follows:

$$|E^*| = \frac{\sigma}{\varepsilon}$$

Where:

$\sigma$  = the amplitude of stress

$\varepsilon$  = the amplitude of strain

In addition, the lag between the load and deformation signal, expressed as a phase angle ( $\phi$ ) is further related to the complex modulus as follows:

$$|E^*| = [E'^2 + E''^2]^{0.5}$$

where:

$$E' = \text{storage modulus} = |E^*| \cos \phi$$

$$E'' = \text{loss modulus} = |E^*| \sin \phi$$

For a pure elastic material,  $\phi = 0$  whereas for a pure viscous materials,  $\phi = 90^\circ$ . Typical values of  $\phi$  for most asphalt mixtures range from  $0^\circ$  to  $60^\circ$ . The testing of dynamic modulus of asphalt mixtures has shown that generally a visco-elastic solid model best describes the performance over a wide range of frequencies and temperatures with the dynamic modulus expressed as a sigmoid function. In this type of model the phase lag typically will vary from 0 to approximately  $60^\circ$ .

### SAMPLE PREPARING AND LABORATORY TESTING

Seven sets of specimens (totally 14 specimens with two replicates per set) were used in this study. The materials being evaluated were made with a series of void contents and are referenced 1 to 7 – with 1 corresponding to the highest void content while 7 has the lowest value. All work was performed at the Asphalt Institute, Lexington, KY.

A standard Kentucky job mix formula (JMF) was blended with 5.4 percent asphalt binder. The aggregate composition was 25 percent limestone #8's, 26 percent limestone sand (unwashed), 14 percent limestone sand (washed), and 15 percent natural sand (rounded). The asphalt binder that was used in this study (PG 64-22) was from a local terminal and used widely in Kentucky. The gravities for the aggregate,  $G_b$ ,  $G_{sb}$ , and  $G_{se}$  were 1.030, 2.68, and 2.724, respectively. The asphalt binder content of 5.4% was optimized using a Superpave 9.5mm coarse-graded mixture design at 75 gyrations and 4.0% air voids.

To fabricate the specimens with different air void levels, the quantity of the materials used to prepare the specimens was varied and a standard compaction height was used. The aggregates and asphalt were mixed and aged according to AASHTO R30, Mixture Conditioning of Hot-Mix Asphalt (Section 7.2, Short-Term Conditioning for Mixture Mechanical Property Testing). The aging and compaction temperature was 135°C (275°F). The mixture was placed into the Superpave Gyratory Compactor (SGC) and set to a 150mm compaction height. The volumetrics of the materials are summarized as shown in TABLE 1. The target air voids for each set was at an increment of  $1.5 \pm 0.3$  percent. The average values of each set are reported throughout the report.

**TABLE 1 Compacted Volumetric Characteristics**

Series Ref.	Air Voids, %	Voids in Mineral Aggregate (VMA), %	Voids filled with asphalt (VFA), %
1	11.3	21.1	46.3
2	9.8	19.8	50.2
3	8.4	18.5	54.6
4	7.1	17.4	58.8
5	5.5	15.9	65.4
6	3.8	14.5	73.4
7	2.3	13.1	82.1

The  $|E^*|$  tests were performed for the seven series (14 specimens – 2 at each void content) at three different temperatures (4, 20 and 40°C) and with nine different frequencies (25, 20, 10, 5, 2, 1, 0.5, 0.2, 0.1 Hz) which is in accordance with AASHTO TP 62-03. The  $|E^*|$  for each test condition is determined through use of the average amplitude of the haversine load from the load cell and the average deformation measured from each axial LVDT. The details on computation of  $|E^*|$  are provided in NCHRP Report 465 (5).

### DATA ANALYSIS

In the proposed “2002 Guide for the Design of Pavement Systems”, the modulus of the asphalt concrete is determined from a master curve constructed at a reference temperature. Master curves are constructed using the principle of time-temperature superposition (see FIGURE 1). The data at various temperatures should be shifted with respect to log of time until the curves

merge into a single smooth function. The resulting master curve of the modulus, as a function of time, formed in this manner describes the time dependency of the material. The amount of shift required at each temperature required to form the master curve describes the temperature dependency of the material.

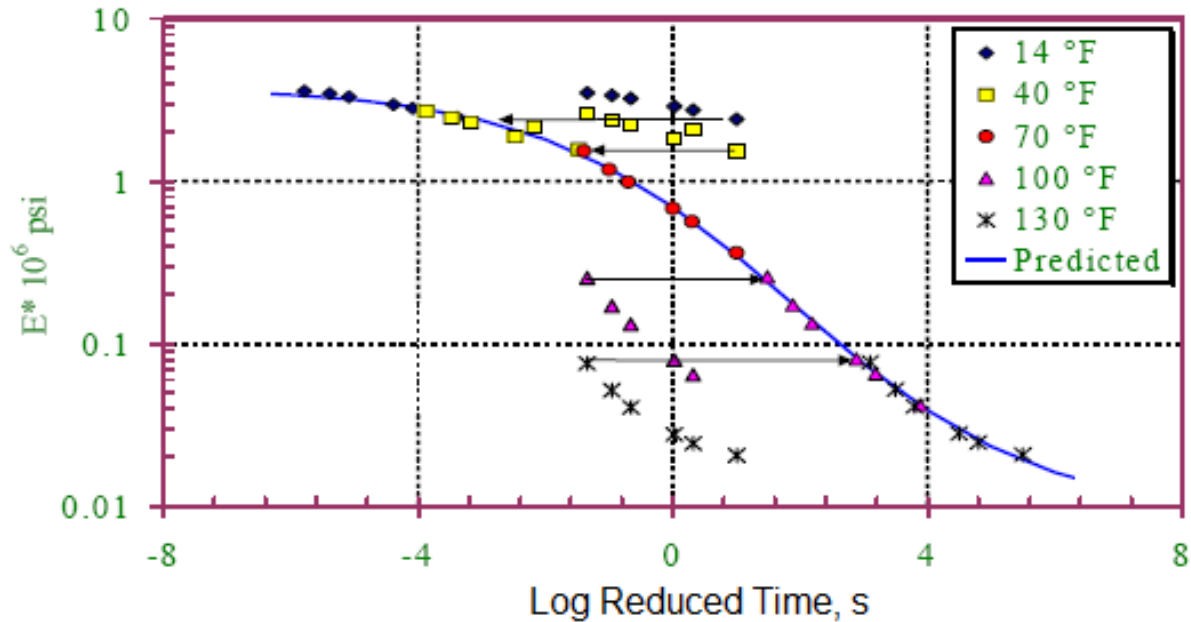


**FIGURE 1** Example of master curve construction in reduced time format (the time is taken to be seconds = 1/frequency) taken from Ref #3.

The master curve within the MEPDG is of a standard sigmoid form which is referenced as Witczak's (symmetrical or standard logistic) Sigmoid, as follows:

$$\log|E^*| = \delta + \frac{\alpha}{1 + e^{\beta + \gamma(\log \omega)}}$$

An alternate sigmoid that can be used is the Richards' ( $\delta$ ) (non-symmetrical or generalized logistic) Sigmoid.

$$\log|E^*| = \delta + \frac{\alpha}{[1 + \lambda e^{\beta + \gamma(\log \omega)}]^{1/\lambda}}$$

Where:

- $\delta$  Lower asymptote, limit for  $|E^*|$  at long loading times and high temperatures
- $\alpha$  Describes upper asymptote,  $(\delta + \alpha)$  gives limit for  $|E^*|$  at short loading times and low temperatures
- $\beta, \gamma, \lambda$  Describes the shape of the sigmoid

The principle advantage of Richards' equation over the standard logistic is that greater flexibility exists in fitting non-symmetric mastercurve data. The non-symmetric behavior is evidenced by an inflection point that is not half distance between the maximum and minimum dynamic complex modulus.

Data has been analyzed using several procedures as follows:

1. Excel-Solver analysis using solver to obtain master curve fits using the Witczak sigmoid function.
2. RHEA™ developed by Rowe and Sharrock (7) was used to produce an analysis with discrete spectra to obtain glassy and equilibrium modulus values and other contributing parameters to the relaxation and retardation spectra.
3. RHEA was further used to determine fits to both Witczak's (standard logistic curve) and the Richard's sigmoid (generalized logistic curve) functions.

The glassy and equilibrium modulus are considered as the asymptotes that are obtained from the various model fits with the glassy modulus corresponding to the higher asymptote and the equilibrium corresponding to the lower asymptote. The values can also be obtained from the fit of a relaxation spectra or retardation spectra for a visco-elastic solid model. In the analysis these parameters have been computed from all three methods defined and presented for comparison.

The parameters associated with the above analysis have all been prepared for a reference temperature of 20°C. In the analysis of data in the RHEA software the shifting was performed using the Gordon and Shaw (8) procedures whereas using the EXCEL program with SOLVER the fitting was done using numerical optimization to the Witczak symmetrical sigmoid model.

## ANALYSIS RESULTS

In the Excel solver analysis, the general form of the dynamic modulus master curve is a modified version of the dynamic modulus master curve equation included in the Mechanistic Empirical Design guide (AASHTO TP 62-03):

$$\log|E^*| = \delta + \frac{(\text{max} - \delta)}{1 + e^{\beta + \gamma(\log \omega_r)}}$$

Where:

- |E\*| = dynamic complex modulus, psi
- $\omega_r$  = reduced frequency, Hz
- Max = limiting maximum modulus (at the glassy condition), psi
- $\beta$ ,  $\delta$ , and  $\gamma$  = fitting parameters

The shift factors at each temperature are given by:

$$\log a(t) = \frac{\Delta E_a}{19.147 \left( \frac{1}{T} - \frac{1}{T_r} \right)}$$

Where:

- a(t) = shift factor at temperature  $T$

$T_r$  = reference temperature, °K  
 $T$  = test temperature, °K  
 $\Delta E_a$  = activation energy

Using this model and the Mastersolver Version 2.0, developed by NCHRP (2), the Witzak parameters and master curves for different air voids are obtained as shown in Table 2 and FIGURE 2. The information plotted in FIGURE 2 has been plotted using a log-normal graph to demonstrate the differences in dynamic modulus at the high end of the scale.

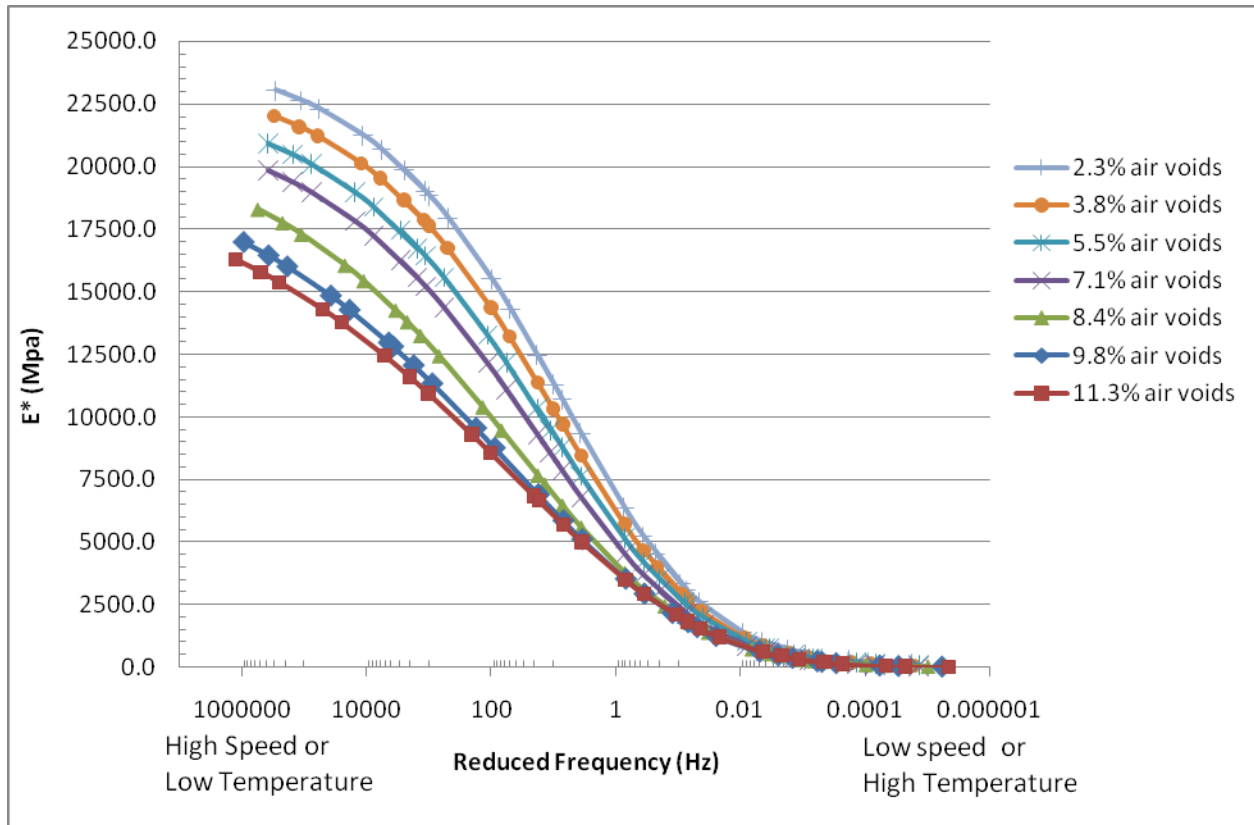


**FIGURE 2 Master curves for different air voids (different series) using Witzak sigmoid function**

**TABLE 2 Witzak Parameters Computed Using Excel and Solver**

Series Ref.	$\Delta E_a$	$\delta$	$\beta$	$\gamma$	Max (Glassy Modulus), MPa	Equilibrium Modulus, MPa	Inflection Point, Hz
1	232015.5	-7.31	-2.63	-0.34	20063.12	0.0395167	1.34E-05
2	225562.7	-3.97	-2.21	-0.37	23058.85	0.0538788	1.77E-05
3	214221	-0.85	-1.62	-0.43	26278.45	0.0484777	1.36E-05
4	206281.1	-0.15	-1.53	-0.50	34241.09	0.0035881	2.08E-06
5	205799.3	-0.24	-1.56	-0.48	28776.23	0.2062729	3.95E-05
6	201568.5	0.37	-1.48	-0.55	36696.7	0.047569	9.57E-06
7	200586.6	0.7	-1.42	-0.57	39042.9	0.051995	6.88E-06

In the RHEA analysis, results are obtained for the glassy and equilibrium modulus obtained from the fitting of a discrete spectra (or Prony series) (Table 3). In addition the results are presented for the two sigmoid formats discussed earlier for the Witczak sigmoid in Table 4 whereas the parameters for the Richard's model are given in Table 5.

**TABLE 3 Equilibrium Dynamic Modulus ( $E_e$ ), Glassy Dynamic Compliance ( $D_g$ ), and Glassy Dynamic Modulus ( $E_g$ )**

Ref	$E_e$ MPa	$D_g$ 1/MPa	$E_g$ MPa
1	6.74E-01	5.83E-05	1.72E+04
2	4.28E+00	5.50E-05	1.82E+04
3	9.63E+00	5.10E-05	1.96E+04
4	1.57E-01	3.87E-05	2.59E+04
5	3.34E+01	4.25E-05	2.35E+04
6	4.73E+01	3.57E-05	2.80E+04
7	2.74E+01	3.16E-05	3.16E+04

**TABLE 4 Witczak Parameters Computed Using the RHEA Software**

Series Ref.	$\alpha$	$\delta$	$\beta$	$\gamma$	Glassy Modulus MPa	Equilibrium Modulus MPa	Inflection Point Hz
1	5.253229	-0.9545273	-1.723188563	-0.3829005	19,893	0.111	3.16E-05
2	4.612674	-0.2491132	-1.641044545	-0.42797	23,097	0.563	1.46E-04
3	3.998142	0.3805879	-1.45154412	-0.4421184	23,918	2.402	5.21E-04
4	5.021598	-0.5319336	-1.590735017	-0.3775729	30,879	0.294	6.12E-05
5	4.193462	0.2361922	-1.555829066	-0.4370865	26,894	1.723	2.76E-04
6	4.168391	0.3567095	-1.521166826	-0.4294803	33,504	2.274	2.87E-04
7	3.980174	0.5470085	-1.515648532	-0.4312255	33,665	3.524	3.06E-04

**TABLE 5 Richard's Parameters for Dynamic Modulus Mastercurve**

Series Ref.	$\alpha$	$\delta$	$\beta$	$\gamma$	$\lambda$	Glassy Modulus MPa	Equilibrium Modulus MPa	Inflection Point Hz
1	4.284639	0.0856861	-1.6263765	-0.36139	0.0269762	23,460	1.218	3.16E-05
2	4.094	0.301216	-1.5136863	-0.39476	0.3657426	24,844	2.001	1.46E-04
3	3.871488	0.5072934	-1.4245677	-0.4339	0.8406166	23,921	3.216	5.21E-04
4	3.406716	1.239363	-1.1996798	-0.28475	0.6532455	44,267	17.353	6.12E-05
5	2.963827	1.5033	-1.2466533	-0.42988	0.001	29,318	31.864	1.26E-03
6	2.932582	1.619395	-1.2307169	-0.42931	0.001	35,643	41.629	1.36E-03
7	3.314477	1.252753	-1.336007	-0.38011	0.088893	36,917	17.896	3.06E-04

## DISCUSSION

### Glassy Modulus

The complex modulus at the glassy condition was analyzed using the various methods as described above. In addition, the aggregate gradation and mixture volumetrics have also been used to determine this parameter. The analysis for three of the cases is illustrated in FIGURE 3 for three methods of analysis versus the prediction method. This data suggests that the MEPDG prediction procedure significantly over-predicts the glassy asymptote. The one data point above the line of equality was for a result that was more difficult to analyze and involved some software modifications for the analysis. It is interesting to observe that the SOLVER and the logistic models in RHEA tend to produce similar results for the glassy asymptote. The discrete spectra appears to produce a lower analysis number compared to the other methods, which can be partly expected since this is a very significant analysis method compared to the functional fitting methods.

The effect of air voids on the glassy modulus is clearly illustrated in Figure 4. The air voids appears to be the best volumetric parameter that describes the variation in the glassy asymptote. However, additional studies may suggest other important volumetric parameters affecting this value.

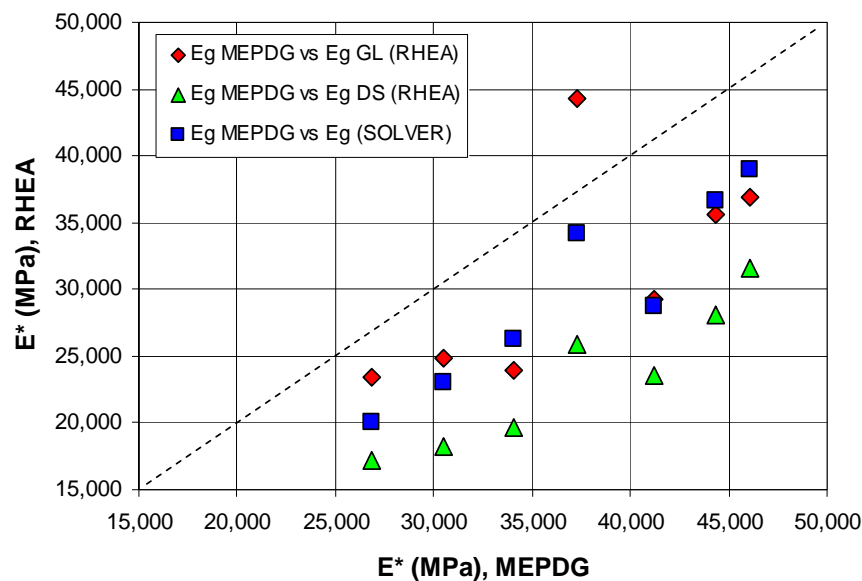


**FIGURE 3 Glassy modulus from the MEPDG prediction equation using mixture properties and computed from test data using RHEA (GL = generalized logistic function, DS = discrete spectra) and EXCEL (with SOLVER)**

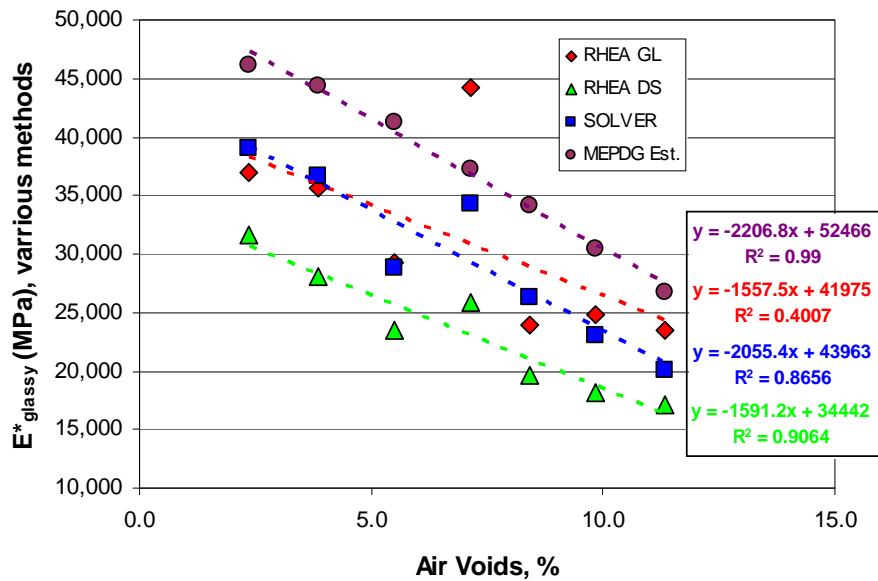


**FIGURE 4 Effect of air voids on the glassy asymptote**

**Equilibrium Modulus**

The value of equilibrium modulus obtained from the different analysis methods differs widely. The ranges obtained are shown in TABLE 6. The values obtained trend in general agreement with the air void contents. The lowest values were obtained using the EXCEL and SOLVER analysis procedure, whereas the highest values were obtained from the data analysis using the RHEA software and Richard’s equation. The values from RHEA using the Witczak equation (standard logistic) give numerical values below that developed from the predicative equation. All of the analysis techniques showed more sensitivity to air void level compared to the predicative equation developed by Witczak as illustrated in FIGURE 5.

**TABLE 6 Equilibrium Modulus Ranges and Average from Various Methods (units = MPa)**

Analysis method	Low Value	High Value	Average
RHEA DS	0.674	47.323	19.765
RHEA GL	1.218	41.629	16.454
RHEA SL	0.111	3.524	1.556
EXCEL and SOLVER	0.004	.206	0.067
Witczak Predication	3.9	6.7	5.443

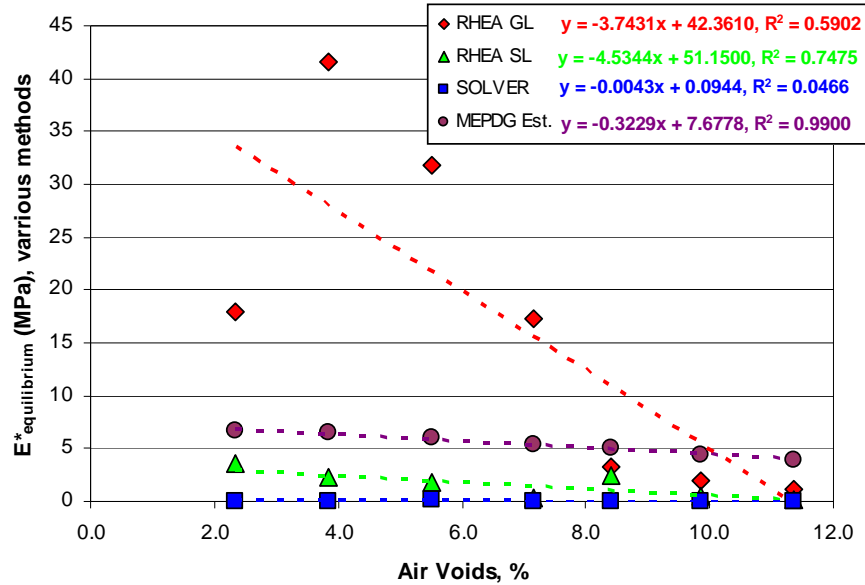


**FIGURE 5 Values of equilibrium modulus versus air void content**

## DISCUSSION

The analysis giving values closest to that predicted from the Witczak predictive approach were the RHEA sigmoid analysis methods. However, it should be noted that the numerical procedures used to fit the Richard's sigmoid require some modifications. It should be noted that the standard sigmoid is a special case of the generalized sigmoid where  $\lambda=1$  as shown by Rowe et al. (9). A significant amount of extrapolation in the data is occurring to define the full sigmoid parameters with all three approaches. Typically the data covers  $2\frac{1}{2}$  decades of stiffness whereas the prediction models define approximately 5 decades of stiffness. The data defines more closely the low temperature properties whereas the more significant extrapolation by the models is taking place at the high temperature end of the testing.

It was noted that the data obtained at the highest test temperature was not fitting the expected phase angle relationship as calculated from the differential of the master curve model form (Rowe, 10) as shown in FIGURE 6. This led to some investigative analysis of the cause of this difference. It was noted during the testing that some permanent deformation of the specimens was taking place and this appears to be related to the void level in the specimen as observed in FIGURE 7. The difference in air voids before and after the  $|E^*|$  test is negligible as shown in FIGURE 8 and was the value of modulus when re-measured at 20°C (see FIGURE 9). The deformation that occurs in the specimen during the high temperature testing (40°C) is clearly evident when inspecting FIGURE 10 through FIGURE 12. In this example it can be seen that from the tests at 25Hz to 2Hz the specimen has deformed by approximately 600 micro-strain. The data then appears to show recovery of the specimen although this is not physically possible with the Haversine loading and additional permanent deformation must be occurring. The apparent recovery is most likely associated with software and/or numerical issues and is currently being investigated further. The specimen is most likely experiencing further deformation consistent with the data in FIGURE 7 which suggest a permanent strain approaching 1500 micro-strain. This level of strain during the  $|E^*|$  test is most likely resulting in non-linear behavior and deviation of the phase angle response from the expected behavior. Due to the high

permanent strain on the modulus samples, one should not further test the same sample as was originally planned with Flow Number testing. New samples that have not been deformed should be used for Flow Number testing.

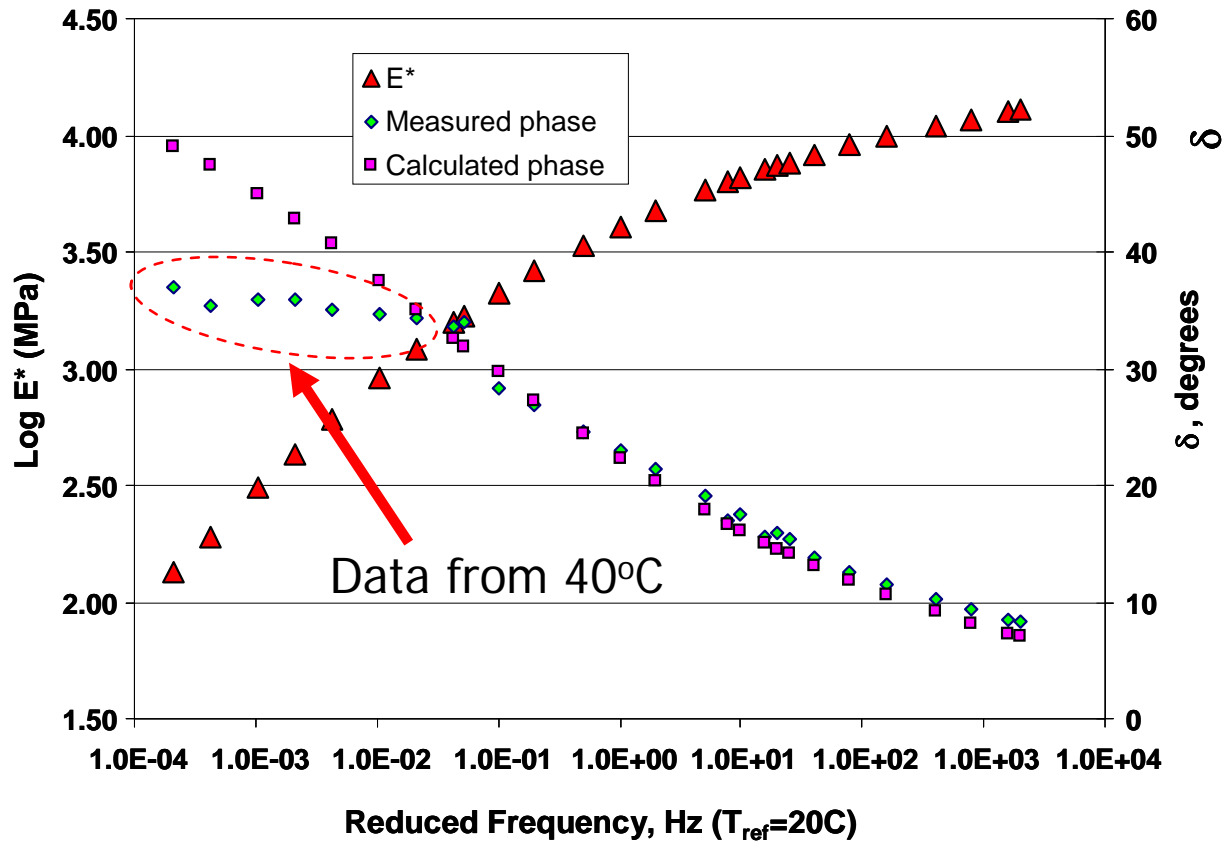


**FIGURE 6** Differences in observed and calculated phase angle using the procedure developed by Rowe (2008) was observed in all materials, with divergent data for the 40°C isotherm

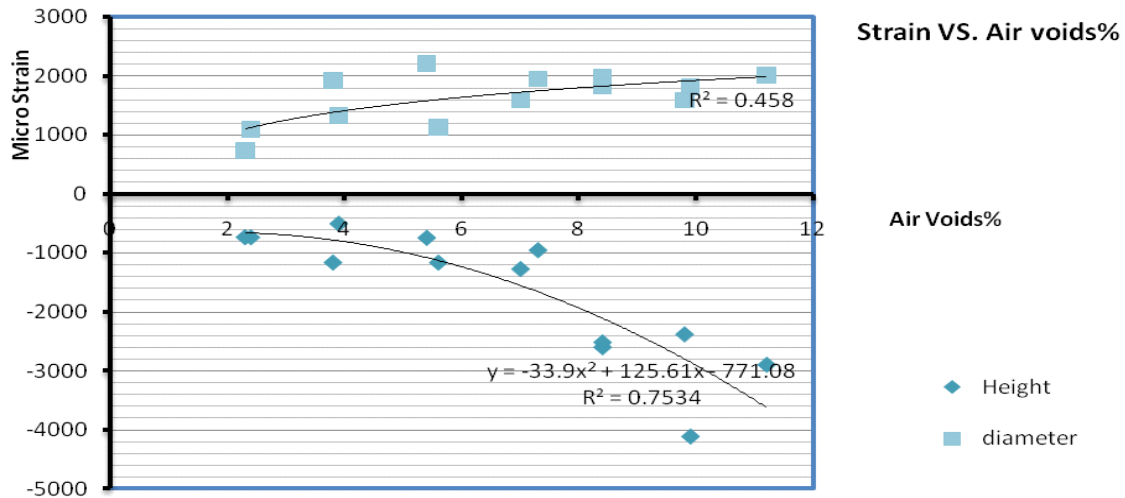


**FIGURE 7** Permanent strains in specimens versus air voids (after SPT test)

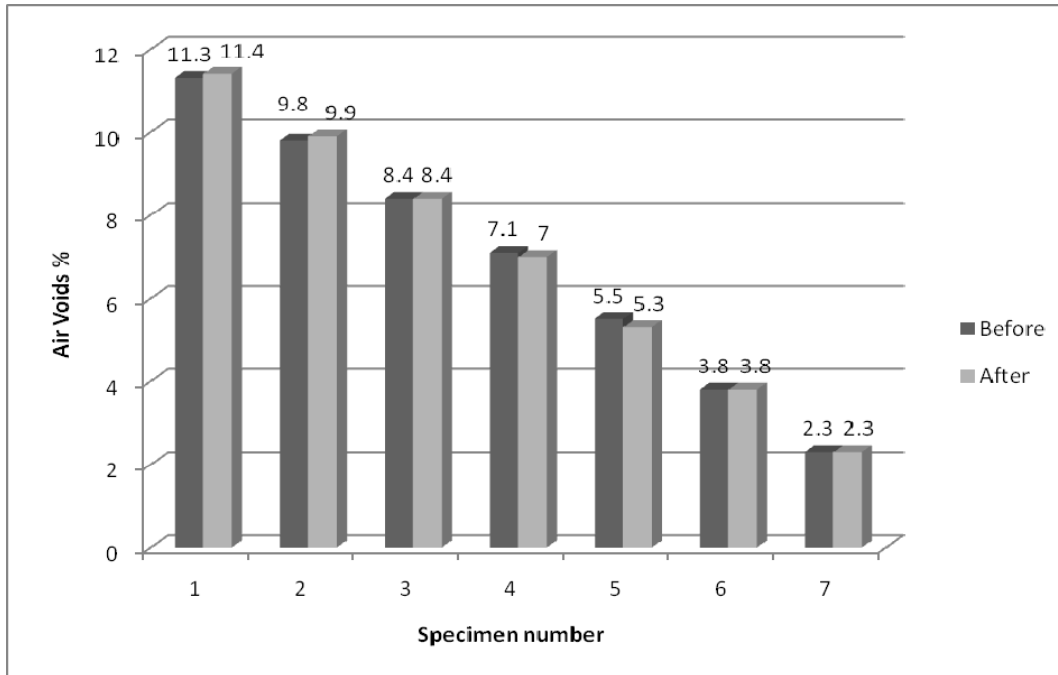


**FIGURE 8** Comparison between air voids of the specimens before and after E\* test

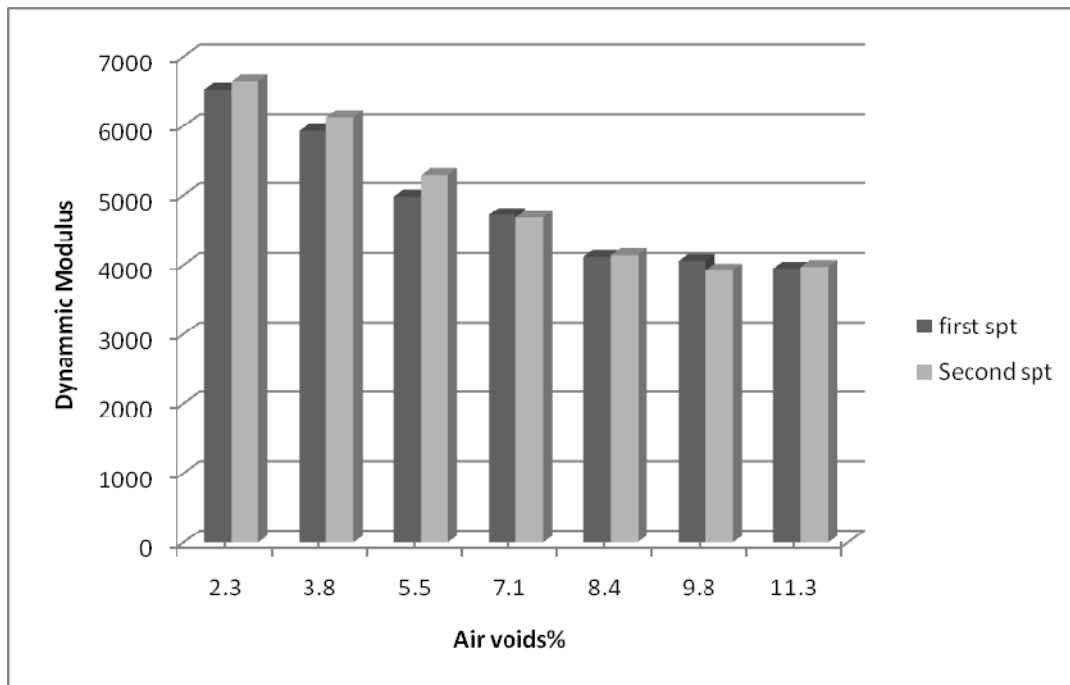


**FIGURE 9** Effect of permanent strain on samples that have been tested using the SPT modulus test, tests conducted at 1 Hertz and 20°C

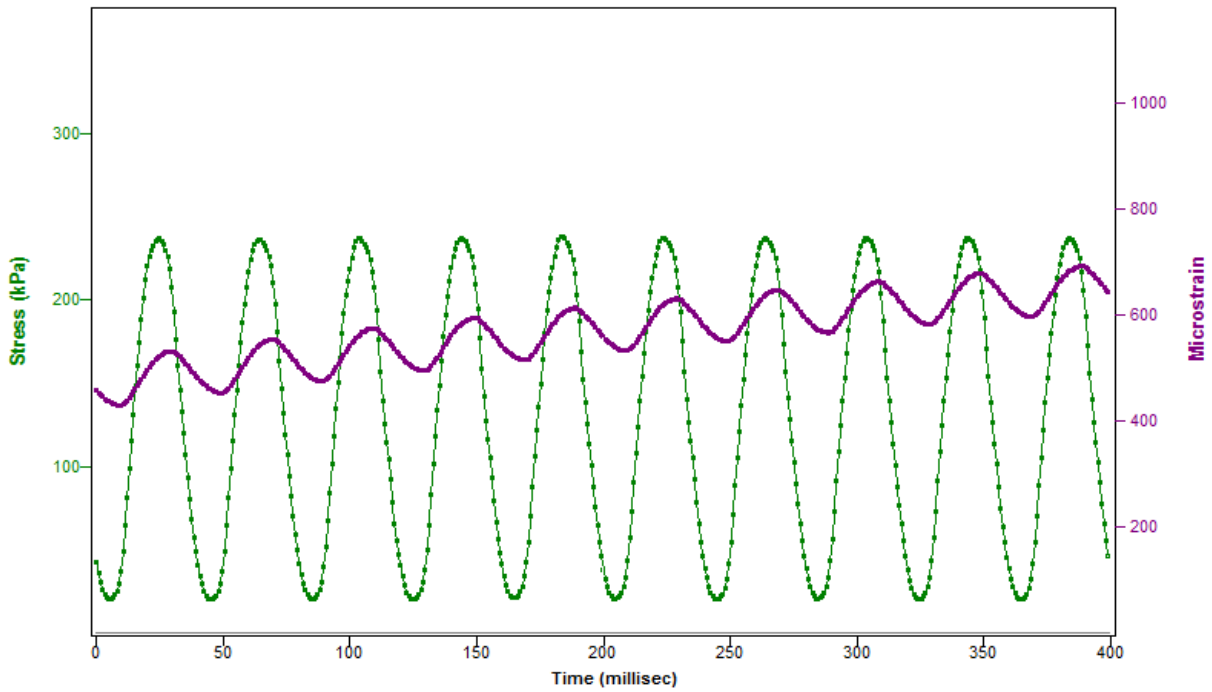


**FIGURE 10** Example of creep in experimental data, specimen 7b, 40°C, 25 Hertz

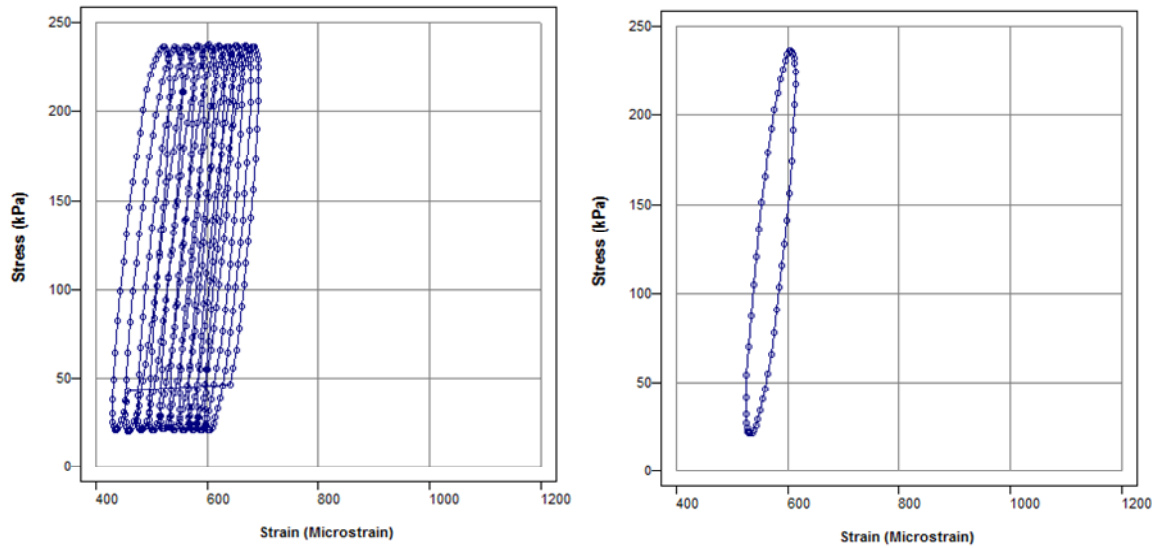


**FIGURE 11** Data from the total hysteresis (left side) was used to produce an average hysteresis loop (right side) for clarity to look at variation of stress and strain during test

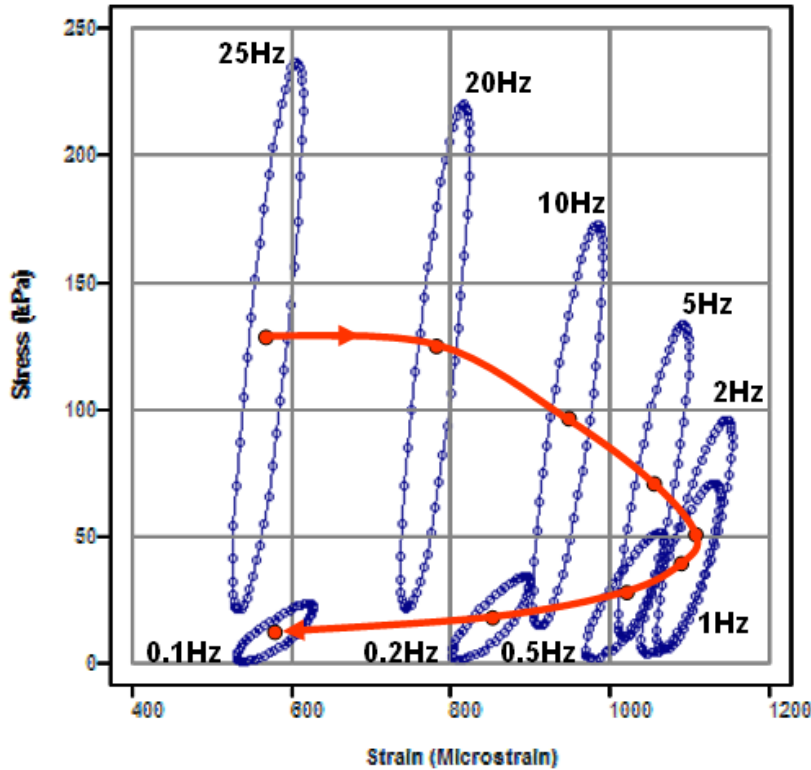


**FIGURE 12** Variation in position of mean hysteresis loop as reported by software for SPT test, specimen 7b, 40°C

## CONCLUSIONS

The results of this analysis lead to the following observations:

1. The values of equilibrium and glassy modulus are significantly affected by the selected analysis method as well as by the volumetric properties of the mixture.
2. The MEPDG prediction procedure significantly over-predicts the glassy asymptote.
3. The phase analysis data obtained from the high temperature testing did not coincide with the expected relationship for this parameter. It is highly likely that large permanent strain is significantly affecting this parameter.
4. Retests of materials properties at 20°C before and after the full frequency sweep data gave very similar results.
5. The permanent strain occurring in any given specimen appears to be significantly affected by the volumetrics. Additional work is required to deduce if this is truly a volumetric effect or a stiffness effect.
6. Dynamic modulus samples that incur this large permanent strain should not be used for further testing. New samples should be made for Flow number testing.

The work presented in this paper is limited to one mixture type, one binder type and content. Consequently, care should be taken when applying these data to other materials. Additional work is recommended to fully understand the cause and effects reported in this paper.

## ACKNOWLEDGEMENTS

The authors gratefully acknowledge the support of the Kentucky Transportation Cabinet and Federal Highway Administration for funding this study. We also want thank the University of Kentucky Transportation Center as the prime contractor of this research. The authors thank the staff at Asphalt Institute especially Shay Emmons and Jason Coleman for their help in preparing the specimens used in this study. The authors also thank Dr. Kamyar Mahboub and Mr. Clark Graves at University of Kentucky for their help in conducting this study and analysis conducted by Mark Sharrock of Abatech International, Ltd. all of whom were a vital part of this program of work.

## REFERENCES

1. Witczak, M. W., and T.K. Pellinen, AC Mixture Response comparison to Performance  $[E^*]$  and Sm Prediction Equation Methodology Results. *Superpave Support and Performance Models Management, Task C: Simple Performance Test. NCHRP Project 9-19*, Team Report SPT-ALF-2(L), Transportation Research Board of the National Research Council, 2000.
2. Bonaquist, R.F., Simple Performance Tester for Superpave Mix Design, *Quarterly Progress Report. NCHRP Project 9-29*. Transportation Research Board of the National Research Council, Washington, D.C., 2003.
3. *Guide for Mechanistic-Empirical Design of New and rehabilitated Pavement Structures. NCHRP 1-37A Project*, Transportation Research Board of the National academies, Washington, D.C., 2003.
4. Witczak, M. W., *NCHRP Report 547: Simple Performance Tests: Summary of Recommended Methods and Database*, Transportation Research Board of the National Academies, Washington, D.C., 2005.
5. Witczak, M. W., T.K. Pellinen, K. Kaloush, M. El-Basyouny, and H. V. Quintus, *NCHRP Report 465: Simple Performance Test for Superpave Mix Design*, Transportation Research Board of the National Research Council, Washington, D.C., 2002.
6. Richards, F. J., A Flexible Growth Function for Empirical Use, *Journal of Experimental Botany*, Vol. 10, No 29, 1959, pp 290-300.
7. Rowe, G.M., and M.J. Sharrock, Development of Standard Techniques for the Calculation of Master Curves for Linear-Visco Elastic Materials, The 1st International Symposium on Binder Rheology And Pavement Performance, The University of Calgary, Alberta, Canada, August 14 - 15, 2000.
8. Gordon, G.V., and M.T. Shaw, *Computer Programs for Rheologists*, Hanser/Gadner Publ., 1994.
9. Rowe, G.M., G. Baumgardner, and M.J. Sharrock, A Generalized Logistic Function to describe the Master Curve Stiffness Properties of Binder Mastics and Mixtures, 45th Petersen Asphalt Research Conference, University of Wyoming, Laramie, Wyoming, July 14-16, 2008.
10. Rowe, G.M., Phase Angle Determination and Interrelationships within Bituminous Materials, 45th Petersen Asphalt Research Conference, University of Wyoming, Laramie, Wyoming, July 14-16, 2008.